ADVANCING EARTH AND SPACE SCIENCES

JGR Atmospheres

RESEARCH ARTICLE
10.1029/2022JD038380

Wave Breaking Events and Their Link to Rossby Wave Packets and Atmospheric Blockings During Southern Hemisphere Summer

Iago Pérez-Fernández[1], Marcelo Barreiro[1], Noémie Ehstand[2], Emilio Hernández-García[2], and Cristobal López[2]

[1]Departamento de Ciencias de la atmósfera y Física de los Océanos, Facultad de Ciencias, Universidad de la República, Montevideo, Uruguay, [2]Instituto de Fisica Interdisciplinar y Sistemas Complejos (IFISC), CSIC-UIB, Palma de Mallorca, Spain

Key Points:

- Large-scale wave breaking events associated to transient long-lived Rossby waves occur more often in the middle-eastern Pacific basin
- Transient Rossby Wave Packets do not cause large-scale wave breaking events that last enough to develop into an atmospheric block
- Near 17% of blocking events appear preceded by a wave breaking event but most of them are not linked to transient Rossby Wave Packets

Correspondence to:

E. Hernández-García,
emilio@ifisc.uib.es

Citation:

Pérez-Fernández, I., Barreiro, M., Ehstand, N., Hernández-García, E., & López, C. (2024). Wave breaking events and their link to Rossby Wave Packets and atmospheric blockings during southern hemisphere summer. *Journal of Geophysical Research: Atmospheres*, *129*, e2022JD038380. https://doi.org/10.1029/2022JD038380

Received 14 DEC 2022
Accepted 10 JAN 2024

Abstract Rossby Wave Packets (RWPs) are atmospheric perturbations located at upper levels in mid-latitudes which, in certain cases, terminate in Rossby Wave Breaking (RWB) events. When sufficiently persistent and spatially extended, these RWB events are synoptically identical to atmospheric blockings, which are linked to heatwaves and droughts. Thus, studying RWB events after RWPs propagation and their link with blocking is key to enhance extreme weather events detection 10–30 days in advance. Hence, here we assess (a) the occurrence of RWB events after the propagation of transient RWPs, (b) whether long-lived RWPs (RWPs with a lifespan above 8 days, or LLRWPs) are linked to large-scale RWB events that could form a blocking event, and (c) the proportion of blocking situations that occur near RWB events. To do so, we applied a tracking algorithm to detect transient RWPs in the southern hemisphere during summertime between 1979 and 2021, developed a wave breaking algorithm to identify RWB events, and searched for blocking events with different intensities. Results show that LLRWPs and the other RWPs displayed large-scale RWB events around 40% of the time, and most RWB events in both distributions last around 1–2 days, which is not long enough to identify them as blocking situations. Nearly 17% of blockings have a RWB event nearby, but barely 5% of blockings are linked to RWPs, suggesting that transient RWPs are not strongly linked to blocking development. Lastly, large-scale RWB events associated with RWPs that lasted less than 8 days are influenced by El Niño-Southern Oscillation.

Plain Language Summary When an atmospheric wave breaks in the upper levels of the atmosphere, it modifies the wind flow in the upper atmosphere and can drastically change local weather conditions. If wave breaking events are sufficiently big and stable, they can produce atmospheric blocking events, which are linked to heatwaves and drought development. Here, we assess whether a link between wave breaking events caused by long-lived traveling atmospheric waves (waves that last more than 8 days in the atmosphere) and blocking event development exists during southern hemisphere summer. Independently of the duration of the wave packets, near 4 out of 10 times they cause very extensive wave breaking events, but do not last long enough time in the atmosphere to be considered an atmospheric blocking. Oppositely, nearly 20% of blocking events manifest nearby a wave breaking event independently of the strength of the block, but these wave breaking events do not seem to be linked to traveling wave packets. Therefore, this study suggests that traveling atmospheric waves are not directly related to the development of atmospheric blockings. Also, the occurrence of extensive wave breaking events caused by traveling atmospheric waves that last less than 8 days is influenced by El Niño-Southern Oscillation.

1. Introduction

Rossby Wave Packets (RWPs) are synoptic scale perturbations that appear in the upper atmosphere of mid-latitudes. During their propagation, these packets travel by downstream development mechanisms, transporting large quantities of energy in the process (Chang & Yu, 1999; Chang, 2000; Yeh, 1949). RWPs play an important role in the global atmospheric circulation because they are related to storm track variability (Souders et al., 2014a). In addition, they are precursors of extreme weather events such as heatwaves, extreme rainfall (Chang, 2005; Grazzini & Vitart, 2015; O'Brien & Reeder, 2017; Wirth et al., 2018) and extratropical cyclone development (Chang et al., 2005; Sagarra & Barreiro, 2020). Also, during their propagation they increase the uncertainty of middle-long range forecast (from 3 to >10 days in advance) in the areas they cross (Zheng

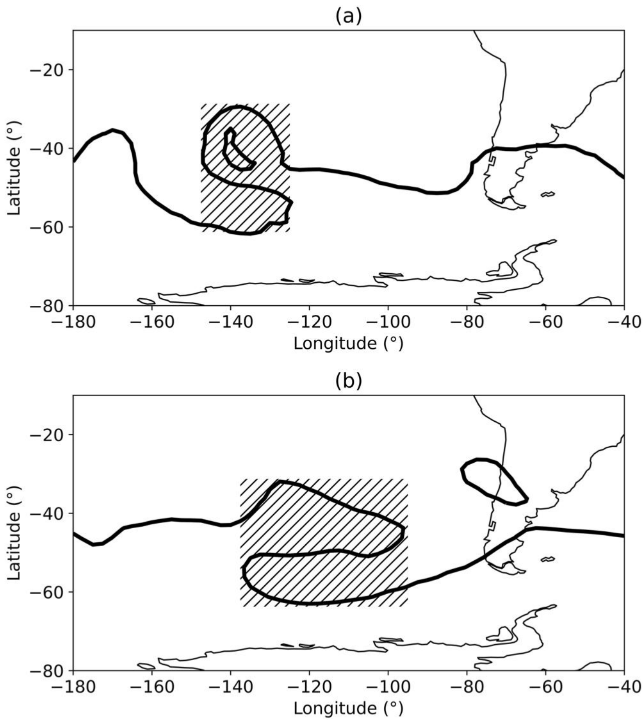

Figure 1. Example of different RWB shear following the −2 PVU units ($m^2 s^{-1} K kg^{-1}$) contour. (a) shows an anticyclonic RWB event detected the 22/12/2000 and (b) a cyclonic RWB event found the 23/12/1991 in the Pacific ocean. Hatched areas identify sections where the potential vorticity fields overturn (isolated contour cells of are not considered part of RWB events).

et al., 2013). Normally, these packets tend to last between 3 and 6 days in the atmosphere but, under certain circumstances, they can last up to 2–3 weeks before disappearing (e.g., Pérez et al., 2021). When RWPs have a lifespan longer than 8 days, they are referred to as long-lived RWPs or LLRWPs (Grazzini & Vitart, 2015).

The lifespan and propagation of the RWPs greatly depend on the potential vorticity gradients in the upper troposphere and the locations of diabatic heating sources (Grazzini & Vitart, 2015). Potential vorticity gradients shape the waveguide where the RWPs propagate, such that a very zonal, intense and narrow jet with strong potential vorticity gradients favor the development of very stable RWPs (Chang & Yu, 1999; Souders et al., 2014b; Wirth, 2020), whereas weaker gradients damp or stop the wave packets propagation (Grazzini & Vitart, 2015).

In the southern hemisphere there are more baroclinically favorable conditions due to the fewer continental areas compared to the northern hemisphere, thus, RWPs in the Southern hemisphere are larger and easier to detect (Grazzini & Vitart, 2015). In addition, during austral summer (December to March) the jet stream displays a very zonal and narrow wind flow, which acts as a waveguide where RWPs propagate (Chang, 1999; Hoskins & Ambrizzi, 1993), and facilitates RWPs detection. Changes in the background conditions that alter the jet stream mean flow also affect RWPs activity. Barreiro (2017) concluded that El Niño events favor RWPs activity. Pérez et al. (2021) found that Southern Annular Mode (SAM) events heavily influence the development of LLRWPs during austral summer, such that years with positive SAM disfavor LLRWPs activity whereas negative SAM favor their development. On the other hand, El Niño-Southern Oscillation (ENSO) influence was found to be less robust.

When RWPs attain large amplitudes, they can reach a critical point in which the crest or trough of the wave overturns, and as a result, the wave packet "breaks", causing an irreversible mixing of potential vorticity fields over a longitudinally confined region (Jing & Banerjee, 2018; McIntyre & Palmer, 1983; McIntyre et al., 1984; Simmons & Hoskins, 1978). As a consequence, high potential vorticity air intrudes the troposphere and/or low potential vorticity air enters in the stratosphere, causing the development of potential vorticity anomalies that can either remove or reverse the usual potential vorticity meridional gradients. This process is called Rossby Wave Breaking or RWB (Berrisford et al., 2007; Masato et al., 2011; McIntyre & Palmer, 1983; McIntyre et al., 1984), RWB usually occurs when the RWPs reach a region where the baroclinic growth is limited (e.g., the continental areas), there the RWPs are affected by a barotropic decay, hence the packets strongly deform and break (Kaspi & Schneider, 2011, 2013; Lee, 1995; Swanson et al., 1997). RWB events are key to the air mass exchange between the troposphere and the stratosphere (Holton et al., 1995), and are considered as potential precursors of weather regime transitions (Michel & Riviére, 2011) that can increase the prediction skill of precipitation (Ryo et al., 2013). In addition, when RWBs have enough spatial extension and last enough time in the atmosphere, they are synoptically recognized as an atmospheric blocking (Berrisford et al., 2007). An atmospheric blocking event is a nearly-stationary large-scale pattern in the pressure field arising from the reversal of the westerly upper tropospheric wind flow, and it is stable enough to last from several days to weeks (Patterson et al., 2019; Rex, 1950). Its appearance is linked to the development of extreme weather events such as heatwaves or droughts (Woollings et al., 2018).

There are two main types of RWB (Thorncroft et al., 1993), one is cyclonic RWB, where low potential temperature or "cold" air from the dynamical tropopause moves eastward and equatorward to the west of high potential temperature air or "warm" air, whereas "warm" air goes poleward and westward. The other is anticyclonic RWB, where the equatorward and westward movement of low potential temperature air is to the east of the poleward and eastward movement of the "warm" air, each morphology of wave breaking implies different changes in synoptic circulation. Figure 1 shows examples of RWB events with anticyclonic (Figure 1a) and cyclonic (Figure 1b) shear. RWB activity is affected by the latitude and location of the storm track, such that cyclonic RWB occurs more often on the polar side of the storm track, whereas anticyclonic shear manifests more often on the equatorward side (Weijenborg et al., 2012). Nonetheless, it has been found that RWB activity in the tropopause is mainly anticyclonic (see Figure 1a) (Peters & Waugh, 1996, 2003; Thorncroft et al., 1993).

Several studies of RWB were done for the Northern Hemisphere (e.g., Masato et al., 2011; Michel & Riviére, 2011; Ryoo et al., 2013; Strong & Magnusdottir, 2008). For example, Thorncroft et al. (1993) found that RWB frequency is influenced by processes that alter the background mean flow in the upper troposphere, such as modes of climate variability. In that regard, Strong and Magnusdottir (2008) concluded that the positive phase of the Northern Annular Mode is associated with anticyclonic RWB, whereas its negative phase is linked to cyclonic RWB. In the southern hemisphere, Berrisford et al. (2007) showed that RWB in mid latitudes wintertime is concentrated in the east Pacific, whereas during summertime RWB episodes are less frequent and are confined to the west Pacific. This is in (qualitative) agreement with the observed location of southern hemisphere blocking. Gong et al. (2010) studied the influence of SAM and ENSO on RWB breaking during austral spring-summer, and found that the positive phase of SAM shows higher wave breaking activity than the negative. Additionally, Wang and Magnusdottir (2010) observed that anticyclonic and cyclonic RWB frequency is affected by the changes in background flow caused by ENSO events.

There are numerous studies about the characteristics and frequency of occurrence of atmospheric blocking events, but there is not yet an accepted unifying theory about the mechanisms involved in the development and onset of an atmospheric blocking (Berrisford et al., 2007; Lupo, 2020; Weijenborg et al., 2012). Rossby (1945) proposed that blocking is the effect of the convergent distribution of group velocity in long quasi-stationary waves. On the other hand, Yeh (1949) suggested that blocking can be explained as the slow energy dispersion of a single wave, and that blocking is a high latitude phenomenon whose intensity and persistence intensifies with the latitude. The latter claim is supported by recent studies, such as Luo (2000), which observed that baroclinic synoptic-scale eddies transform the blocking event from a dispersive to a non-dispersive system in its onset, whereas the opposite occurs in the decay of the blocking. Other studies also suggested that extratropical RWPs that propagate in mid latitudes are able to interact with the background flow, affecting atmospheric blocking formation (Hoskins and Sardeshmuk, 1987; Renwick & Revell, 1999). Additionally, Nakamura et al. (1997) showed that synoptic scale transient eddies are important for the formation and maintenance of blocking events that occur in the North Pacific region. Also, Nakamura and Huang (2018) discuss the onset and maintenance of blocking by studying the convergence of wave activity flux, suggesting that blocking events occur when the jet stream is oversaturated with wave activity, blocking the usual wind and energy flux.

Other studies have assessed the link between RWB and atmospheric blocking events. Berrisford *et al.* (2007) stated that persistent large-scale wave breaking occurring in the atmosphere is a strong indicator that blocking event might be present. Nonetheless, as reported by Hitchman and Huesmann (2007) not all RWB events are necessarily linked to atmospheric blocking, such as small scale or transient scale RWB events. On the other hand, Weijenbrog et al. (2012) showed that most blocking events that occur in the North-Atlantic and Europe are caused by anticyclonic breaking Rossby waves, while Rodrigues and Woolings (2017) proposed that Rossby waves that break anticyclonically in South America during austral summer are responsible for causing blocking events in subtropical South America.

Therefore, previous studies suggest that transient RWPs may be linked to atmospheric blocking development. Nonetheless, to date there are no studies that assess the link between transient RWPs and the onset and development of atmospheric blocking. Another question still unanswered is the relationship between the occurrence of RWB and the propagation of RWPs in the southern hemisphere, as well as whether RWPs can cause RWB events that trigger atmospheric blocking development. Hence, the aim of this research is to study the detection and evolution of RWB events after the propagation of transient RWPs, with special emphasis on large-scale RWB. In addition, we classify the RWB considering whether their associated RWPs are LLRWPs or not, because we are interested in understanding the processes that may increase prediction beyond the synoptic time scale. Lastly, we study whether RWB events that occur after the dissipation of all RWPs are linked to the development of atmospheric blockings.

The paper is organized as follows. Section 2 describes the datasets and the methodologies for tracking RWPs, and detecting RWB events and blockings. Section 3 focuses on the link between RWB and RWPs, Section 4 on the interannual variability of RWB events and the potential impact of global climate modes, and Section 5 assesses the link between atmospheric blocking and RWB events. Finally, Section 6 presents a summary of the study.

2. Data and Methodology

2.1. Data

In this study, we used daily mean data from the ERA 5 Reanalysis (Hans et al., 2020), with an horizontal resolution of 0.25° × 0.25°. The region of study consists of the mid-latitudes of the southern hemisphere, during austral summer (December to March) between 1979 and 2021 as done in previous studies (Pérez et al., 2021; Sagarra & Barreiro, 2020). Thus, we have 41 seasons available for the analysis.

RWPs propagate in the upper atmosphere of mid-latitudes and manifest as meanders of the jet stream. During their propagation, they produce a series of troughs and ridges that travel confined to a certain latitudinal band, moving mainly eastward during austral summer (Chang, 1999). Thus, by computing the envelope of the meridional wind speed at 300 hPa ($V_{300\mathrm{env}}$), we can characterize these transient RWPs. To calculate the $V_{300\mathrm{env}}$, we followed the methodology specified in Pérez et al. (2021) that can be summarized as follows: (a) we compute the daily anomalies by removing the daily mean climatology, and then subtract the seasonal mean variability from the data; (b) we apply the fast Fourier transform and retain wavenumbers that represent atmospheric transients in the southern hemisphere (i.e., waves with wavenumbers between 4 and 11, as in Trenberth, 1981); (c) we then use the inverse Fourier transform to the filtered data obtaining $V_{300\mathrm{env}}$. Finally, due to the fact that RWPs propagation is mostly zonal, and around 50°S in the upper troposphere during December–March season (Chang, 1999), we averaged the $V_{300\mathrm{env}}$ data between the latitudinal range of 40–65ºS.

Regarding the detection of RWB events, as in previous studies, we have used the potential vorticity field in isentropic coordinates. The computation of the potential vorticity field was performed following Hoskins et al. (1985), using daily mean temperature and wind speed at 200, 250, 300 and 350 hPa levels and interpolated them to the isentropic coordinates of 330ºK. In the case of atmospheric blocking detection we used geopotential height at 500 hPa, as in Tibaldi and Molteni (1990).

Also, to characterize the interannual variability and amplitude of the global climate modes, we used the Oceanic Niño Index for ENSO, and the Antarctic Oscillation index for SAM. Both datasets are publicly available in the NOAA website (https://origin.cpc.ncep.noaa.gov/).

2.2. Description of RWP Tracking Algorithm

The RWPs are detected using a tracking algorithm, based on the maximum envelope technique (Grazzini & Vitart, 2015; Pérez et al., 2021; Sagarra & Barreiro, 2020). This algorithm searches for areas with the highest daily values of $V_{300\mathrm{env}}$ in the longitudinal sector. It identifies the center of activity of the RWPs as the point where the value of $V_{300\mathrm{env}}$ is the largest, and then follows the propagation of the wave packets to the east, assuming that they travel between 15 and 45ºE per day. Before applying the tracking algorithm, we filter out small values of $V_{300\mathrm{env}}$ to avoid tracking noise. Although there is no optimum threshold because there are no physical properties that separate one wave packet from another (Souders et al., 2014b), here we applied a minimum threshold of 19 m/s. Pérez et al. (2021) show that the tracking of RWPs is not sensitive to the choice of threshold between 17 and 21 m/s.

The described tracking algorithm only follows transient RWPs, that is, RWPs that propagate eastwards and have a zonal wavenumber between 4 and 11, which correspond to the transient structures of the southern hemisphere (Trenberth, 1981). Therefore, the algorithm cannot track stationary RWPs, or those RWPs with a wavenumber ≤3. Hereafter, when we talk about RWPs, we are referring to these transient RWPs.

After the algorithm finishes tracking all the RWPs of the season, it uses proximity criteria to link trajectories of the RWPs that were interrupted, and then measures the characteristics of the tracked wave packet: longitudinal extension, areas of formation/dissipation, lifespan and propagation speed. The full description of the algorithm is available in Pérez et al. (2021). Finally, for the subsequent analysis, the tracked RWPs are classified in LLRWPs (lifetime >8 days) and short-lived RWPs or SLRWPs (lifetime ≤ 8 days).

2.3. Rossby Wave Breaking Detection Algorithm and Validation

RWB events manifest in the upper atmosphere in areas where the usual meridional gradient of potential vorticity either disappears or reverses, these areas can be located by searching where the potential vorticity contour lines overturn following isentropic coordinates (McIntyre & Palmer, 1983). Previous studies in the southern hemisphere followed potential vorticity contours in the isolines between 310 and 350ºK (Ndarana and Waugh 2010a,

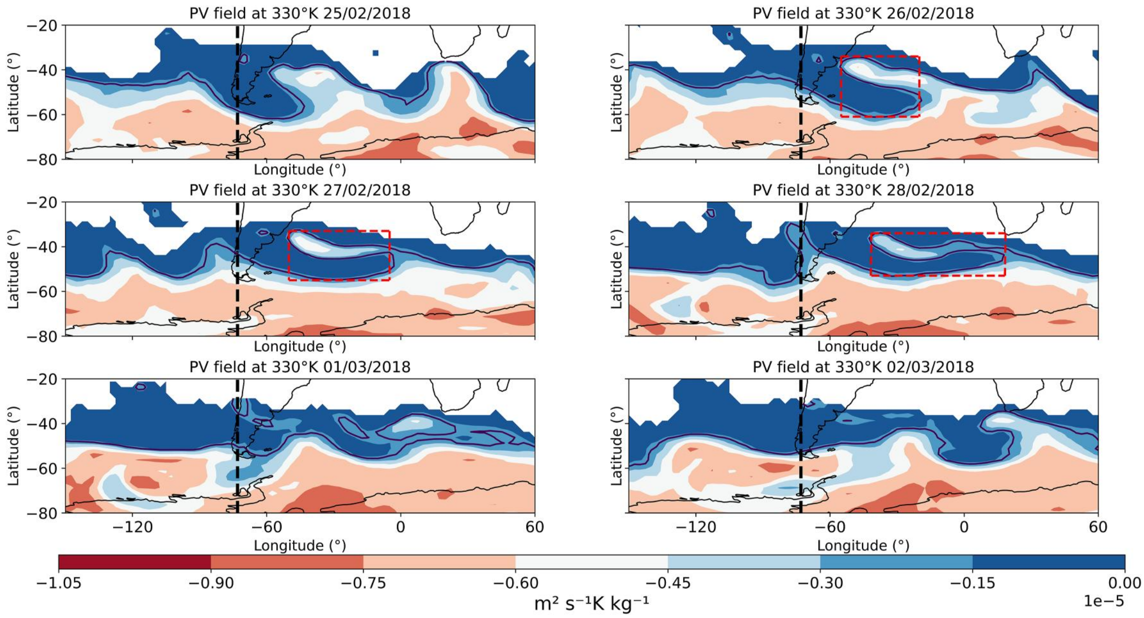

Figure 2. Potential vorticity fields following the 330ºK isosurface between 25/02/2017 and 01/03/2017. The black contour line signals the location of the -2PVU contour line while the dashed black line shows the longitudinal section where a LLRWPs stopped its propagation on 25/02/2017. The red rectangles indicate the area where the wave breaking algorithm detected a large-scale RWB event linked to the RWP that stopped propagating.

201b, Strong & Magnusdottir, 2008) because they represent the dynamical tropopause between the high latitudes and the subtropics (Ndarana and Waugh 2010a). Having this in mind, we developed an objective tracking algorithm able to search the overturning of potential vorticity contours on the 330ºK isosurface, following the isoline of −2 PVU (1 PVU = 10^{-6} m^2 s^{-1} K kg^{-1}). We chose this specific isosurface because it is a transitional region between the upper troposphere and the lower stratosphere in the mid-latitudes of the southern hemisphere, and where most anticyclonic and cyclonic shear have been found (Ndarana and Waugh, 2010a, 2010b).

The RWB tracking algorithm follows the methodology of Barnes and Hartmann (2012), and the steps of the algorithm are the following.

1.- Representation of the −2 PVU contour line for day t, and retention of the longest contour line. This is done to avoid the detection of isolated potential vorticity "bubbles" as part of RWB events (see Figure 1).
2.- Identification of areas where −2 PVU contours crosses more than 2 times the same longitudinal section. These points are referred to as wave breaking points.
3.- If there are wave breaking points closer than 500 km from each other we assumed that these points belong to the same wave breaking event (Barnes & Hartmann, 2012).
4.- Retention of RWB events that have a longitudinal extension ≥ 5°. This avoids registering meridionally extended potential vorticity tongues that do not show overturning.
5.- Classification of the RWB event regarding their orientation. This is done by measuring the latitudinal mean of the 4 most eastward and westward overturning points of the RWB episode. In the southern hemisphere, cyclonic RWB events have their western-most overturning point located equatorward, while their east-most overturning point is poleward. By contrast, in anticyclonic RWB events their eastern-most overturning point are equatorward whereas their west-most overturning point are poleward. Thus, if the latitudinal mean of their most westward points of the contour is closer to poleward latitudes than the observed at the most eastward points, we assume that the wave packet shows an anticyclonic shear, whereas if the most westward points are closer to the equator than the most eastward points, the breaking event is classified as cyclonic RWB. An example of the application of the RWB tracking algorithm can be seen in Figure 2.
6.- Measurement of the RWB characteristics: longitudinal and latitudinal extension of the event, day of detection, and type of RWB shear.

Given the few studies reported on RWB for the southern hemisphere it is important first to ensure that the detection algorithm works as expected. To do so, we first tracked wave breaking events in the December-March

10.1029/2022JD038380

season only between 1979 and 2008, and compared our results against previous studies (Ndarana and Waugh 2010a, 2010b; Wang & Magnusdottir, 2010). The results are shown in Section 3.1.

2.4. Linking Large-Scale Rossby Wave Breaking Events to RWPs

In this section we explain the methodology used to link RWB activity to the dissipation of RWPs. The authors were not able to find a study which links RWB events with RWPs in the southern hemisphere, and propose the following methodology to link RWP with RWB activity. Before describing the methodology, it is important to highlight that from this section onward, we will only consider large-scale RWB, that is, RWB events with a longitudinal extension of 1,000 km (∼15° in mid latitudes) or above (Barnes & Hartmann, 2012). This is done in order to retain wave breaking events that can strongly affect the large-scale atmospheric circulation and have a spatial scale similar to atmosphere blocking (11° of extension, Patterson et al., 2019). It is also important to highlight that we search for large-scale RWB events that occur within 4 days after the RWP stops propagating. The upper limit of 4 days was chosen after examining the evolution and behavior of several potential vorticity fields several days after the dissipation of a RWPs, where we observed no RWB activity 4 days after the packet stopped propagating (see Section 3.2 for a more detailed discussion). The time scale of 4 days may be related to the fact that RWPs can become stationary for a few days before disappearing.

The methodology used for linking RWPs with RWB events has the following steps.

1.- Apply the RWB tracking algorithm at day T_{f}, being T_{f} the day when a RWP finished its propagation.
2.- If the algorithm detects the geographical center of a large-scale RWB event between $X_{\mathrm{f}} \pm 2{,}000$ km, being X_{f} the longitudinal section where the algorithm located a RWPs before stopping its propagation, we assume that the wave breaking event registered is linked to the RWP that stopped its propagation and we proceed to step 3. If the described condition is not fulfilled, we continue looking for RWB events for the following days. If by day $T_{\mathrm{f+4}}$ we do not find a RWB event that matches the described condition, we assumed that the RWP did not show a RWB episode and finish the search. Oppositely, if after applying the wave breaking detection algorithm we detect two or more RWB event which are in the range $X_{\mathrm{f}} \pm 2{,}000$ km, we select the RWB events whose geographical center is closer to the area of dissipation of the RWP.
3.- We register the day when a RWB event is detected as $T_{\mathrm{n,}}$ and applied the RWB tracking algorithm at day $T_{\mathrm{n,+1}}$. If a RWB event exists with geographical center within 20° (∼1,400 km) of distance or less from the wave breaking episode found at day $T_{\mathrm{n,}}$, we assume that this event is an extension of the RWB event found the previous day. Else, we infer that the RWB episode only lasted for a day.
4.- Step 3 is repeated for the following days until we stop finding wave breaking events that fulfill the condition.
5.- We save the same characteristics of the RWB events detailed in Section 2.3 as well as the day a RWB event was detected after the dissipation of a RWP, and how many days lasts the RWB associated to a RWP.

In step 2, we search for RWB events in the area located between $X_{\mathrm{f}} \pm 2{,}000$ km because even if X_{f} signals the center of the RWP, the packet has a certain longitudinal extension, and thus the RWB event does not have to necessarily appear near X_{f}. Barnes and Hartmann (2012) considered that RWB events that are within 2,000 km of the geographical center of the RWB belong to the same episode, hence, in this study we look for RWB events that are up to 2,000 km of distance from the area of dissipation of the RWPs.

Additionally, in step 3 we used a distance of 1,400 km to search for the continuation of a RWB episode, because using a longer distance can cause the algorithm to select a wrong wave breaking event that is too far away from the original episode that is being tracked.

Figure 2 shows an example of the methodology followed to link RWPs with RWB events.

2.5. Linking Atmospheric Blocking to Large-Scale Rossby Wave Breaking Events

Lastly, we compared the proportion of large-scale RWB events that are present nearby the development of an atmospheric blocking event. In order to detect the occurrence of atmospheric blocking events, we use the methodology of Tibaldi and Molteni (1990)—TM90 hereafter, but modified to consider a range of latitudes in the southern hemisphere following Mendes et al. (2011). This technique measures two geopotential height meridional gradients from a central latitude, one to the north (GHGN) and another one to the south (GHGS) by using expressions 1 and 2.

$$\mathrm{GHGN} = \left(Z(\lambda, q_1) - Z(\lambda, q_N)\right) / \left(|q_1 - q_N|\right) \tag{1}$$

$$\mathrm{GHGN} = \left(Z(\lambda, q_s) - Z(\lambda, q_2)\right) / \left(|q_s - q_2|\right) \tag{2}$$

where, $q_N = 40°S + \Delta$, $q_2 = 50°S + \Delta$, $q_1 = 55°S + \Delta$, $q_S = 65°S + \Delta$

Z(λ,q) is the geopotential height at 500 hPa in a latitude q and longitude λ, and Δ belongs to the set {-10,-7.5, −5, −2.5, 0, 2.5, 5, 7.5, 10}. If on a specific day, at a given longitude λ, GHGN >0 and GHGS < −10 m/degree of latitude for, at least, one value of Δ, the longitude is considered to be "blocked". Note that, we measure GHGN and GHGS using slightly different expressions from Mendes et al. (2011), which implies a stronger requirement on the gradients to consider a longitude blocked.

Once instantaneous, local, blocked conditions have been identified, additional persistence and spatial extension requirements must be imposed to define atmospheric blocking events. Various thresholds have been used in the literature. Patterson et al. (2019) define an atmospheric blocking event when they detect a blocked longitudinal sector covering, at least, 11° and when this condition persists for a minimum of 4 days in the atmosphere. Mendes et al. (2011), use a minimum spatial extent of 7.5° in longitude and persistence of 5 days. In our study, we registered events that have a minimum longitudinal extension of 7.5, 10, 12.5, and 15° and display a minimum lifespan of 4–5 days, measuring the longitude of detection, lifetime and zonal extension of the blocks. This is done in order to assess whether the proportion of atmospheric blocks that might be linked to RWB is sensitive to the blocking conditions. Hence, events that last at least 4 days with a longitudinal extension of 7.5° are most frequent and represent blocking-like situations, that is, the persistent reversal of the westerly upper troposphere wind flow that are not sufficiently extensive to be considered as a blocking event, whereas those that last more than 5 days and have a zonal extension of at least 15° are considered the strongest blocks of the dataset.

In addition to the index described above, there exist a large variety of indices for the detection of atmospheric blocking events. These indices complete each other by capturing different features of blocks -we refer to Woolings et al. (2018), Barriopedro et al. (2010), Lupo (2020) for comprehensive reviews. Nonetheless, the most commonly employed methodology is the TM90 one. In particular, in the southern hemisphere, where much fewer blocking studies exist compared to the northern hemisphere, this has been by far the prevailing approach (Damiâo and Machado, 2008; Damião et al., 2012; Mendes et al., 2011; Toulabi Nejad et al., 2022). The choice of TM90 in our work, therefore allows us to verify the correctness of the algorithm outputs by comparison with previous studies. Our choice is further motivated by the effectiveness of this index for the detection of omega blocks and ridges with a marked meridional axis tilt (Pinheiro et al., 2019), which are typically observed in dipole blocks and wave breaking situations. This characteristic along with the flexibility offered by the wide range of latitudes covered (Δ) and variation of spatio-temporal criteria makes our index well suited for studying the co-occurrence of large-scale RWB events and atmospheric blocking events.

In Section 3, we first verify that our algorithm works as intended by measuring the frequency of occurrence and areas of formation of blocking events in our period of study, comparing the results to those obtained in Mendes et al. (2011). We then study the potential links between large-scale RWB events and blocking events by identifying the events which occur on the same day and such that their respective geographical center are separated by a maximum of 2,000 km. The fulfillment of the latter conditions ensures that the RWB event is present near the development of the atmospheric block. Lastly, we determine how many of the RWB events that occur near an atmospheric block are associated to propagating RWPs. This analysis assesses the proportion of atmospheric blocks that are associated to large-scale RWB activity, and whether RWB activity linked to propagating RWPs is directly linked to the development of atmospheric blocking events.

3. Rossby Wave Breaking Events and Their Relationship to RWPs

3.1. Verification of Rossby Wave Breaking Algorithm

The analysis of RWB events during the December-March season between 1979 and 2008 detected a total of 659 RWB events in December, 470 in January, 413 in February and 581 events in March. As for the orientation of the RWB events, 22% of the total wave breaking activity belongs to cyclonic RWB, and 78% to anticyclonic RWB. Thus, RWB activity detected is mainly anticyclonic, as reported by Thorncroft et al. (1993) and Peter and

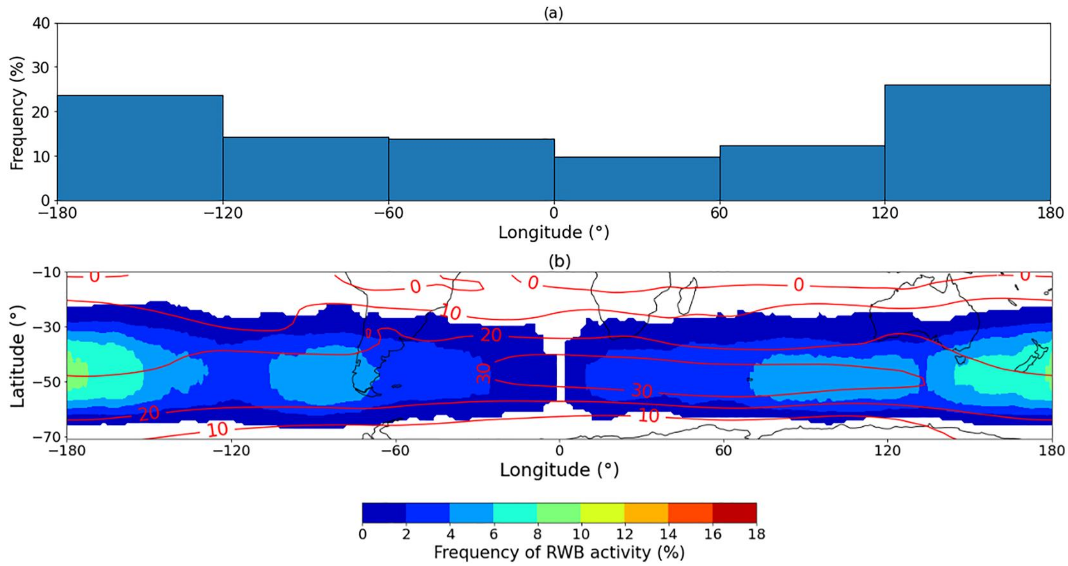

Figure 3. Frequency of total RWB events (a) and anticyclonic RWB activity (b) found during summertime in the Southern Hemisphere between 1979 and 2008. Shading in (b) indicates anticyclonic RWB frequency (in %) f and red lines the mean zonal wind speed at 300 hPa (in m/s).

Waugh (2003). Our results are in agreement with those obtained in Ndarana and Waugh (2010a, 2010b) as shown below.

Figure 3a shows the longitudinal distribution of RWB frequency of occurrence independently of its shear. The maximum RWB activity occurs in the eastern Indian Ocean (between 120ºE and 180ºE) followed by the western Pacific (−180ºE-120ºE), and the lowest activity is located in the Atlantic (near 0ºE–60ºE). These results indicate that RWB is weakest at the jet entrance in the Atlantic basin, and largest at the jet exit, consistent with the fact that largest RWP activity occurs in the Atlantic-Indian basin where the strong jet acts as waveguide (Pérez et al., 2021).

Additionally, Figure 3b shows the areas of anticyclonic RWB activity. The main area of anticyclonic RWB detection is located in the western Pacific, as reported by Ndarana and Waugh (2010b). Nonetheless, we also observe two secondary areas of maximum anticyclonic RWB activity, one located in the Indian Ocean and the second in the eastern Pacific-western Atlantic. The latter is in agreement with Ndarana and Waugh (2010b), but these authors found very little anticyclonic RWB activity in the Indian Ocean during December–February. Nonetheless, Ndarana and Waugh (2010b) found significant anticyclonic RWB activity in that region during March–May, suggesting that the differences with our results are explained because of our consideration of March in the summer season. Thus, overall our results are close to those observed in Ndarana and Waugh (2010b), providing a verification of our RWB algorithm. In our case the areas of RWB frequency have wider meridional extension than those found in Ndarana and Waugh (2010b), because our algorithm registers the whole latitudinal area where the overturning potential vorticity is detected.

3.2. Characteristics of Rossby Wave Breaking After RWP Propagation

For the southern hemisphere summertime during 1979–2021, a total of 1,256 RWPs were found, which corresponds to around 30 per season. Moreover, 141 were LLRWPs, that is about 11% of the total RWPs. From the 141 LLRWPs, 45% have associated large-scale RWB, whereas for the SLRWPs (1,115 cases) this proportion is close to 39%. In both cases RWB events show mainly anticyclonic shear: 79% (76%) of the RWB episodes detected after the propagation of a LLRWP (SLRWP) show anticyclonic RWB.

Figure 4 displays the frequency of occurrence per longitude of large-scale RWB events as a function of longitude that happened after the end of LLRWPs or SLRWPs as well all large-scale RWB that happened after the end of any RWP, independently of their lifespan. When we focused on large-scale RWB events linked to the end of LLRWPs propagation (Figure 4a), we found that most of these events mainly occur between −120ºE and −60ºE (eastern Pacific basin). On the other hand, large-scale RWB events associated to SLRWPs and to all RWPs

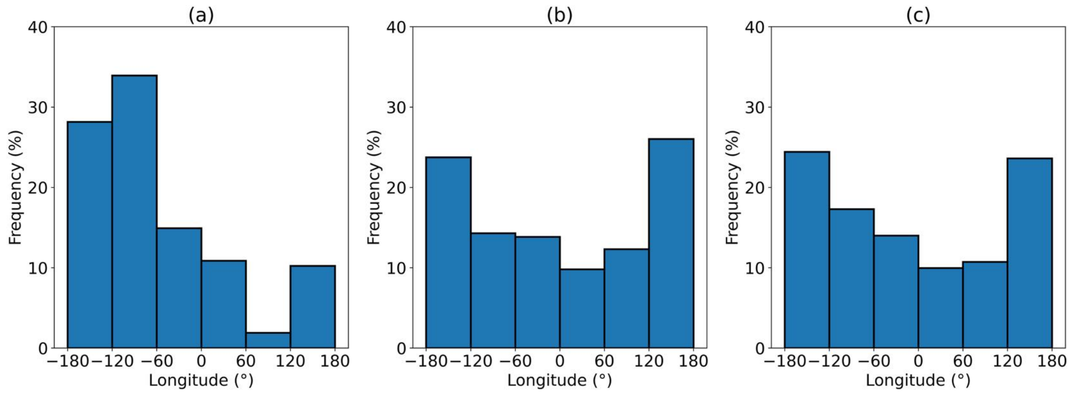

Figure 4. Relative frequency of occurrence of large-scale RWB associated to (a) LLRWPs, (b) SLRWPs, and (c) all RWPs during austral summer 1979–2020.

(Figures 4b and 4c), mainly occur in the region between 120ºE to 180ºE (eastern Indian basin), in agreement with Ndarana and Waugh (2010a). As expected, Figures 4b and 4c show very similar distributions because SLRWPs represents around 90% of the all RWPs.

These results thus show that large-scale RWBs associated to LLRWPs are eastward displaced compared to RWBs associated with the rest of the packets. This is consistent with Perez et al. (2021), who showed that LLRWPs propagation is modulated by SAM, and that during negative SAM, when LLRWPs occur more often, the waveguide where RWPs propagate is extended into the Pacific. Thus, this suggests that when LLRWPs propagate, they travel further east and break in the Pacific ocean, instead of in the eastern Indian ocean sector. Hence, large-scale wave breaking events associated with LLRWPs tend to occur in the middle-eastern Pacific basin, which could imply that long-lived packets might be precursors of weather regime transitions affecting conditions in South America.

The temporal and spatial characteristics of large-scale RWB events detected after the dissipation of LLRWPs and SLRWPs are considered next. Figures 5a and 5d display the number of days that pass until a RWB event is detected after the dissipation of a SLRWPs or a LLRWP, respectively. The two distributions are similar, that is, most of the RWB events occur on the same or the next day after the RWPs stop propagating, and barely any wave breaking activity is detected 3 days after. Additionally, Figures 5b and 5e show the lifespan of the RWB events linked to SLRWPs/LLRWPs, indicating that most of the large-scale RWB linked to RWPs last between 1 and 2 days, and that there are no significant differences between distributions. Nonetheless, when we compare the zonal extension of the wave breaking events (Figures 5c and 5f), we found that RWB events that occur after the propagation of SLRWPs usually cover larger longitudinal extensions compared to those observed after LLRWPs. RWB events linked to LLRWPs show a median longitudinal extension of 22°, and a interquartile range of 12°, whereas RWB associated with SLRWPs have a median of 26.5° and display an interquartile range of 15°. A Kruskall-Wallis test applied to the datasets of Figures 5c and 5d, indicates that the distributions are significantly different, at 5% level of significance.

Hence, these results suggest that RWB events caused by SLRWPs cover larger longitudinal extensions of the atmosphere compared to those produced by LLRWPs. Nonetheless, neither LLRWPs or SLRWPs seem to be directly related to atmospheric blocking development because, even if the associated large-scale RWB events have similar spatial scales to a blocking event, they tend to last only about 1–2 days, too short to lead to blocking (see also Section 5).

4. Interannual Variability of Rossby Wave Breaking Events Associated to LLRWPs/SLRWPs

Perez et al. (2021) reported a negative correlation between SLRWPs and LLRWPs, such that during years with high LLRWPs activity, SLRWPs occur less often. Therefore, one might expect a negative correlation between the number of RWB events associated with LLRWPs and SLRWPs. Figure 6 displays the interannual variability in the occurrence of RWB associated with LLRWPs and SLRWPs. Both time series show large year-to-year

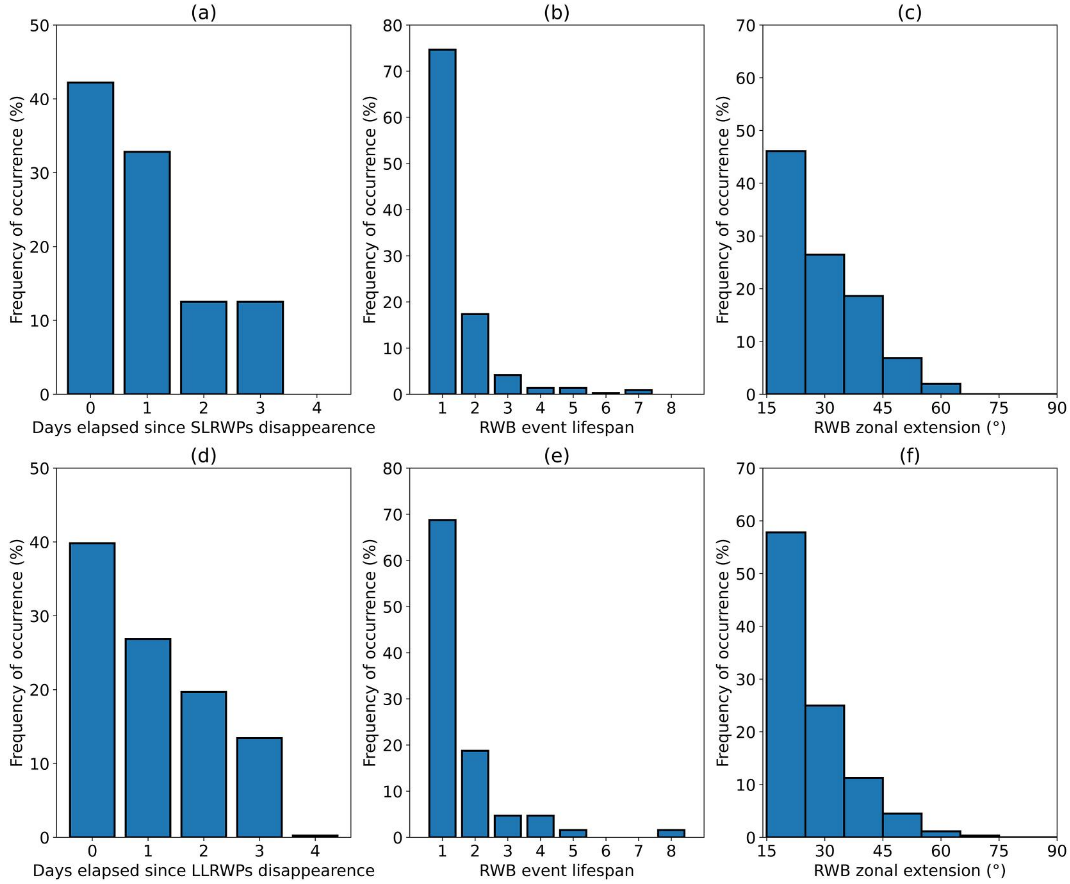

Figure 5. Histogram distribution of several characteristics of RWB associated with LLRWPs (lower panels) and SLRWPs (upper panels). Panels (a) and (d) represent the number of days passed when a large-scale RWB event appears after the end of the SLRWPs or LLRWPs propagation, respectively (day 0 is the same day the wave packet stopped propagating). Panels 5b and 5e display the lifespan of the RWB linked to SLRWPs and LLRWPs. Lastly, panels (c) and (f) show the longitudinal extension of the RWB.

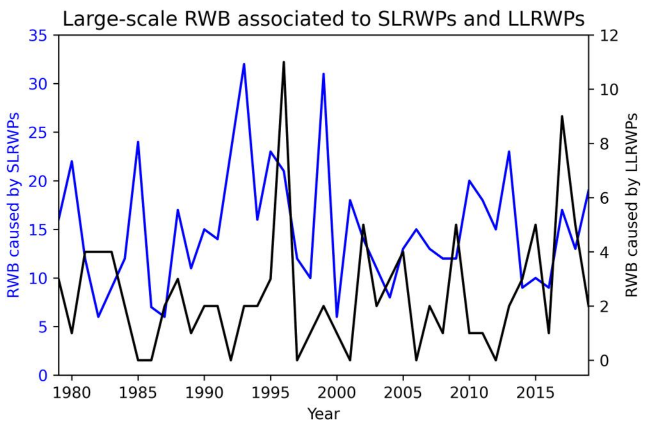

Figure 6. Interannual variability of RWB events associated to LLRWPs (black line) and SLRWPs (blue line) during the period of study.

variability. In the case of LLRWPs, the number of annual RWB events range from 0 to 11, while for SLRWPs it ranges from 6 to 32. During certain periods the frequency of occurrence of RWB associated with the LLRWPs and SLRWPs seem to be out of phase, but no significant correlation has been found between the two time series.

Figure 7 shows the dependency of the frequency of occurrence of large-scale RWB events linked to SLRWPs and LLRWPs with the SAM/ENSO indices, this is, the Antarctic Oscillation Index for SAM (SAM index) and the Oceanic Niño Index (ONI) for ENSO. When we focus on large-scale RWB linked to LLRWPs (Figures 7a and 7b), in both cases the correlation values are close to 0 (∼0.12). Thus, there is no linear relationship between the number of RWB events linked to the dissipation of LLRWPs with SAM or ENSO.

Figures 7c and 7d show the interannual variability of RWB events linked to SLRWPs as a function of SAM/ONI indices. Years with La Niña have a higher frequency of occurrence of RWB linked to SLRWPs, and the opposite occurs in years with El Niño, with a Spearman correlation coefficient value of −0.36 statistically significant at 5% level (using Student *t*-test). Thus, La Niña years tend to favor the development of RWB events, whereas El Niño years

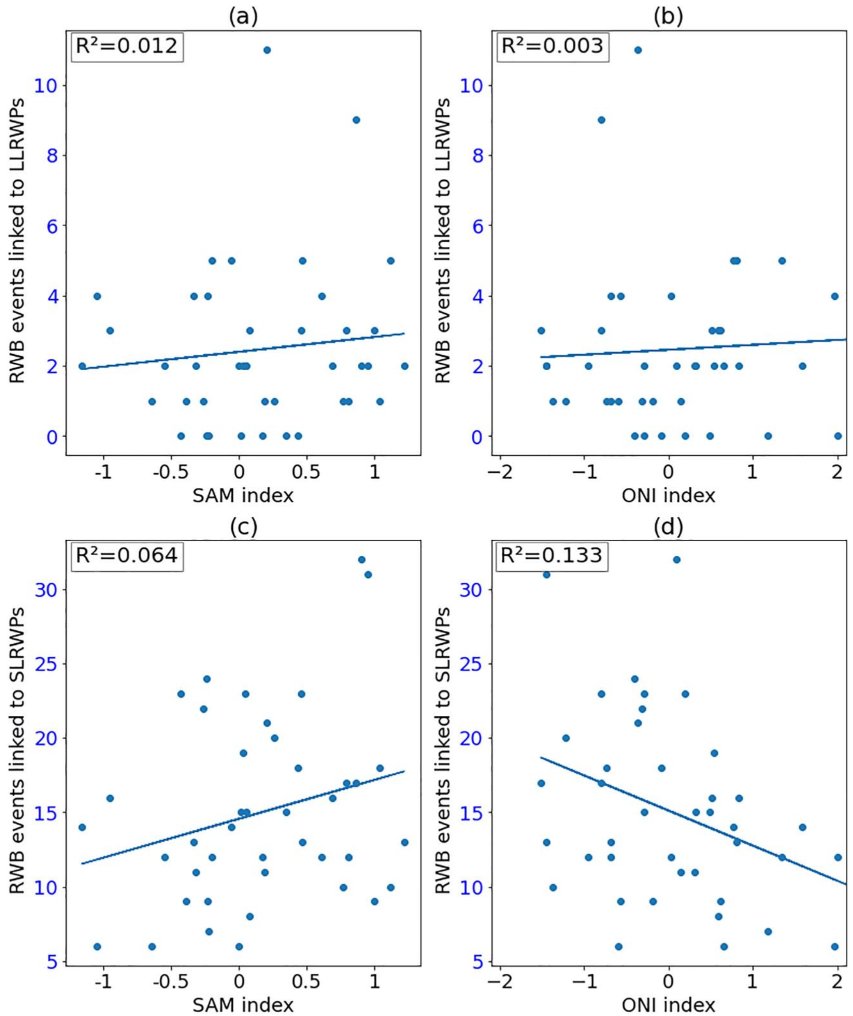

Figure 7. Scatterplot of RWB events linked to LLRWPs (a), (b) and SLRWPs (c), (d) against SAM/ENSO indexes. The lines show an adjusted linear regression with the corresponding determination coefficient (R^2) indicated in each panel.

do the opposite, but the small variance indicates that there are other processes that control interannual wave breaking variability. In the case of large-scale RWB linked to SAM, we obtain a Spearman correlation coefficient value of 0.21, but it is not statistically significant (using Student t-test). In agreement, Wang and Magnusdottir (2010) and Gong et al. (2010) concluded that RWB in the tropical/subtropical Pacific is increased during La Niña events, and this was associated to a strong local decrease in the upper-tropospheric zonal wind. At the same time Barreiro (2017) found that El Niño events tend to favor the RWPs propagation. Therefore, El Niño seems to induce large scale background conditions that favor the propagation of RWPs and, by extension, diminishes the occurrence of RWB, whereas the upper tropospheric wind flow decrease during La Niña disfavors the propagation of RWPs and propitiate the occurrence of RWB events.

5. Link Between Atmospheric Blocking and Large-Scale Rossby Wave Breaking

Results of Section 3.2 suggest that the link between RWB associated with RWPs and blocking is not obvious because these RWB events tend to last 1 or 2 days. Here we look further into the relationship between RWB and blockings.

Table 1 shows the number of blocking events found as a function of the persistence and longitudinal extension considered. For the less restrictive

Table 1
Number of Blocking Events Found Using Different Criteria, (d) Refers to Minimum Lifespan in Days and (L) the Minimum Longitudinal Extension in Degrees of the Atmospheric Blocks Detected

	7.5°L	10ºL	12.5ºL	15ºL
4d	263	212	168	123
	7.5°L	10ºL	12.5ºL	15ºL
5d	142	107	79	55

Table 2
Number of Summertime Blocking Events Between 1979 and 2020 in the Area of Study for Two Blocking Detection Criteria: (d) Refers to Minimum Lifespan of the Event in Days, and (L) to Its Minimum Longitudinal Extension in Degrees

	Eastern south-Atlantic-western Indian basin (0ºE–60ºE)	Central Indian basin (61ºE–120ºE)	Eastern Indian basin (121ºE–180ºE)	Western Pacific basin (−179ºE to −120ºE)	Eastern Pacific basin (−119ºE to −60ºE)	Western South-Atlantic (−59ºE to 0ºE)
4d 7.5° L	10	16	63	118	38	18
5d 15° L	1	2	20	27	4	1

criteria (blocks that last at least 4 days and with a minimum longitudinal extension of 7.5°) there are 263 events between 1979 and 2020 summertime, which corresponds to around six blocking events per season. This large number of events reflects the fact that these criteria cause the finding of more blocking-like situations than atmospheric blocks. On the other hand, for the most intense blocks (lifespan of 5 or more days and with a minimum extension of 15°) there are 55 events, this is, a mean of 1.3 events per year. As expected, we observe a decrease in blocking events as the conditions become more restrictive. We find a mean of 3 atmospheric block events per year when we follow the criteria of Mendes *et al.* (2011), which is similar to the number they found (between 2.9 and 3.1 events per year).

In addition, when we focus on the detection areas of blockings, we find that near 50% of the events appear at the central-western Pacific basin (−180ºE to −120ºE) independently of the zonal extension and persistence of the event. On the other hand, there is a secondary area of blocking development in the eastern Indian basin (121ºE–180ºE), where we find around 23%–38% of the blocking events, showing the highest (lowest) values during the strongest (weakest) blocking events. Oppositely, we barely detect any blocking in the western south-Atlantic (−60ºE to 0ºE) or the central Indian basin (0ºE-60ºE). These results are summarized in table 2 and are in accordance with the observations in Mendes *et al.* (2011).

The search for large-scale RWB associated to the formation of an atmospheric block reveals that the latter appear close to a RWB event between 15% and 18% of the times independently of the strength and stability of the block (not shown). Also, in agreement with the results of Section 3.2, we only found RWB linked to propagating RWPs near the development of an atmospheric block around 3%–6% of the times, and it does not seem to depend on the intensity and stability of the block.

To summarize, RWB events are present in the atmosphere around 1 out of 5 times an atmospheric block is detected, but these RWB events do not seem to be related with propagating RWPs. Thus, propagating RWPs do not seem to be directly linked to the development of atmospheric blocks. We recall that here we described propagating RWPs as those with speed between 15 and 45°/day eastward, a zonal number between 4 and 11, and lifespan larger than 3 days. Therefore, it is possible that planetary RWPs (those with wavenumber between 1 and 3) and quasi-stationary RWPs (RWPs with zonal wavenumber above 4 and speeds <15°/day), which were not considered in this study, might play a key role in the development of atmospheric blocking. One possibility is that atmospheric blocking onset depends on the interaction between transient and stationary waves. In Nakamura and Huang (2018), they stated that periods with high Rossby wave activity can saturate the capacity of the jet to transmit waves, impeding the propagation of oncoming waves and triggering blocking development. They also discussed that transient and stationary wave activity, among other factors, affect the capability of the jet to transport Rossby waves. Thus, further studies should try to address if quasi-stationary and transient RWPs are linked with atmospheric blocking development, being by RWB activity or by other dynamical processes.

Additionally, it is possible that transient RWPs might influence atmosphere blocking by other dynamical processes that are not related to wave breaking activity. For example, through recurrent RWPs: in this mechanism several transient RWPs propagate in such a manner that the troughs and ridges that build up the wave packets are repeatedly amplified at the same longitudes, thus producing unusually persistent surface weather conditions during their lifespan (Barton et al., 2016; Davies, 2015; Röthlisberger et al., 2019).

Alternatively, quasi-stationary or planetary waves might play a larger role in blocking development. Previous studies have found that under certain circumstances, planetary and quasi-stationary synoptic-scale packets resonate together, causing slow-speed synoptic scale Rossby waves amplification, favoring extreme weather events development in the northern hemisphere during boreal summer (Coumou et al., 2014; Kornhuber et al., 2017). Coumou et al. (2014) also suggested that a similar process might happen in the southern hemisphere, but this has not yet been studied.

Therefore, results obtained in this study suggest that there is no direct link between propagating RWPs and atmospheric blocking development, at least, by wave breaking processes. Nonetheless, we cannot rule out the possibility that propagating RWPs might interact with atmospheric blocking events by other dynamical mechanisms and further research is needed.

6. Summary

Rossby Wave Breaking events are atmospheric perturbations that interfere in the upper troposphere wind and energy flow, and under certain circumstances they can cause an atmospheric block, leading to the development of heatwaves or droughts. In this work, an algorithm to track overturning regions of potential vorticity was developed in order to identify Rossby Wave breaking areas that are linked to the dissipation of transient RWPs.

We found that both long-lived RWPs and short-lived RWPs tend to show large-scale wave breaking events around 40% of the time, although this number is slightly higher for long-lived packets. Large-scale Rossby Wave breaking events that occur preceded by long-lived RWPs tend to manifest at the center-eastern part of the Pacific basin, and are less zonally extended compared to the wave breaking events associated with the rest of the packets. Therefore, changes in weather regime conditions caused by wave breaking events that are linked to long-lived RWPs are more likely to occur at the south of South America. Moreover, wave breaking events linked to RWPs tend to last between 1 and 2 days in the atmosphere for both long-lived and short-lived packets. Thus, wave breaking events produced by propagating RWPs do not seem to be directly linked to the development of atmospheric blocks.

Previous studies have found that negative SAM years are characterized by a larger number of long-lived RWPs due to the extension of the Atlantic-Indian basin jet wave guide into the Pacific (Pérez et al., 2021). Here, we report that the frequency of wave breaking linked to long-lived RWPs does not seem to be affected by SAM nor ENSO. On the contrary, La Niña events favor the development of wave breaking episodes after the propagation of short-lived RWPs. Hence, it is suggested that Rossby Wave Breaking activity linked to RWPs is more common during years with La Niña.

Finally, we assessed whether Rossby wave breaking events appear near the development of atmospheric blocks, and found that around one out of 5 times a blocking event develops, a Rossby Wave Breaking event is present. However, large-scale Rossby Wave Breaking linked to propagating RWPs does not seem to be associated with atmosphere blocking development, at least by wave breaking processes. Therefore, blocking event development associated with wave breaking activity during southern hemisphere summertime might be linked to stationary RWPs, or propagating wave packets with very low wavenumber (1–3). Another possibility is that propagating Rossby waves might affect atmospheric blocking development, but through other dynamical processes that are not related by wave breaking activity, such as by the development of recurrent Rossby waves. Further study is needed to address these questions.

Data Availability Statement

ERA5 reanalysis data are freely available in the Copernicus Climate Data Store, whereas ENSO and SAM indexes are available at NOAA website. The wind envelope amplitude of the RWPs used in this study is deposited in a Zenodo repository and publicly available as Perez. I (2021) Wind envelope at 300 hPa in the Southern Hemisphere during austral summer between 1979 and 2020 (Version 1.1) [Dataset]. A datanote describing the mentioned dataset as well as the methodology applied to obtain wind envelope data from meridional wind speed can be found in Pérez and Barreiro (2023), which is publicly available in Open Research Europe.

Acknowledgments

This project has received funding from the European Union's Horizon 2020 research and innovation programme under the Marie Skłodowska-Curie grant agreement No 813844 (ITN CAFE). NE, CL and EHG acknowledge grant PID2021-123352OB-C32 funded by MCIN/AEI/10.13039/501100011033 FEDER/UE.

References

Barnes, A. E., & Hartmann, L. D. (2012). Detection of Rossby wave breaking and its response to shifts of the midlatitude jet with climate change. *Journal of Geophysical Research*, *117*(D9), D09117. https://doi.org/10.1029/2012JD017469

Barreiro, M. (2017). Interannual variability of extratropical transient wave activity and its influence on rainfall over Uruguay. *The international journal of meteorology*, *37*(12), 4261–4274. https://doi.org/10.1002/joc.5082

Barriopedro, D., García-Herrera, R., & Trigo, R. M. A. (2010). Application of blocking diagnosis methods to General Circulation Models. Part I: A novel detection scheme. *Climate Dynamics*, *35*(7–8), 1373–1391. https://doi.org/10.1007/s00382-010-0767-5

Barton, Y., Giannakaki, P., Von Waldow, H., Chevalier, C., Pfahl, S., & Martius, O. (2016). Clustering of regional-scale extreme precipitation events in southern Switzerland. *Monthly Weather Review*, *144*(1), 347–369. https://doi.org/10.1175/MWR-D-15-0205.1

Berrisford, P., Hoskins, J. B., & Tyrlis, E. (2007). Blocking and rossby wave breaking on the dynamical tropopause in the southern hemisphere. *Journal of the Atmospheric Sciences*, *64*(8), 2881–2898. https://doi.org/10.1175/JAS3984.1

Chang, E. K. M. (1999). Characteristics of wave packets in the upper troposphere. Part II: Seasonal and hemispheric variations. *Journal of the Atmospheric Sciences*, *56*(11), 1729–1747. https://doi.org/10.1175/1520-0469(1999)056<1729:cowpit>2.0.co;2

Chang, E. K. M. (2000). Wave packets and life cycles of troughs in the upper troposphere: Examples from the southern hemisphere, summer season of 1984/1985. *Monthly Weather Reviewer*, *128*(1), 25–50. https://doi.org/10.1175/1520-0493(2000)128<0025:wpalco>2.0.co;2

Chang, E. K. M. (2005). The impact of wave packets propagating across Asia on Pacific cyclone development. *Monthly Weather Review*, *133*(7), 1998–2015. https://doi.org/10.1175/MWR2953.1

Chang, E. K. M., & Yu, D. B. (1999). Characteristics of wave packets in the upper troposphere. Part I: Northern Hemisphere winter. *Journal of the Atmospheric Sciences*, *56*(11), 1708–1728. https://doi.org/10.1175/1520-0469(1999)056<1708:cowpit>2.0.co;2

Coumou, D., Petoukhov, V., Rahmstorf, S., Petri, S., & Schellnhuber, H. J. (2014). Quasi-resonant circulation regimes and hemispheric synchronization of extreme weather in boreal summer. *Proceedings of the National Academy of Sciences*, *111*(34), 12331–12336. https://doi.org/10.1073/pnas.1412797111

Damiâo, C. M.-C., Cavalcanti, A. F. I., & Herdies, L. D. (2012). Southern hemisphere atmospheric blocking diagnostic by ECMWF and NCEP/NCAR data. *Rebista Brasileira de Meteorologia*, *27*(3), 263–271. https://doi.org/10.1590/s0102-77862012000300001

Damiâo, C. M.-C., Machado, T. R., Cavalcanti, I. F. A., & DaCamara, C. C. (2008). Blocking episodes in the southern hemisphere: Impact on the climate of adjacent continental areas. *Pure and Applied Geophysics*, *165*(9–10), 1941–1962. https://doi.org/10.1007/s00024-008-0409-4

Davies, C. H. (2015). Weather chains during the 2013/2014 winter and their significance for seasonal prediction. *Nature Geoscience*, *8*(11), 833–837. https://doi.org/10.1038/ngeo2561

Gong, T., Feldestein, B. S., & Luo, D. (2010). The impact of ENSO on wave breaking and southern annular mode events. *Journal of the Atmospheric Sciences*, *67*(9), 2854–2870. https://doi.org/10.1175/2010JAS3311.1

Grazzini, F., & Vitart, F. (2015). Atmospheric predictability and Rossby wave packets. *International Journal of the Royal Meteorological. Society*, *141*(692), 2793–2802. https://doi.org/10.1002/qj.2564

Hans, H., Bell, B., Berrisford, P., Hirahara, S., Horány, A., Muñoz-Sabater, J., et al. (2020). The ERA5 global reanalysis. *Royal Meteorological Society*, *146*(730), 1999–2049. https://doi.org/10.1002/qj.3803

Hitchman, H. M., & Huesmann, S. A. (2007). A seasonal climatology of Rossby wave breaking in the 320–2000-K layer. *Journal of the Atmospheric Sciences*, *64*(6), 1922–1940. https://doi.org/10.1175/JAS3927.1

Holton, J. R., Haynes, H. P., McIntyre, E. M., Douglass, R. A., Roodm, B. R., & Pfister, L. (1995). Stratosphere–troposphere exchange. *Review of Geophysics*, *33*(4), 403–439. https://doi.org/10.1029/95RG02097

Hoskins, J. B., & Ambrizzi, T. (1993). Rossby wave propoagation on a realistic longitudinally varying flow. *Journal of the Atmospheric Sciences*, *50*(12), 1661–1671. https://doi.org/10.1175/1520-0469(1993)050<1661:rwpoar>2.0.co;2

Hoskins, J. B., & Sardeshmukh, P. D. (1987). A diagnostic study of the dynamics of the northern hemisphere winter of 1985-86. *Quarterly Journal of the Royal Meteorological Society*, *113*(447), 759–778. https://doi.org/10.1002/qj.49711347705

Hoskins J, B., McIntyre E, M., & Robertson W, A. (1985). On the use and significance of isentropic potential vorticity maps. *Quarterly Journal of the Royal Meteorological Society*, *111*(470), 877–946. https://doi.org/10.1002/qj.49711147002

Jing, P., & Banerjee, S. (2018). Rossby wave breaking and isentropic stratosphere-troposphere exchange during 1981–2015 in the northern hemisphere. *Journal of Geophysical Research: Atmospheres*, *123*(17), 9011–9025. https://doi.org/10.1029/2018JD028997

Kaspi, Y., & Scheneider, T. (2013). The role of stationary eddies in shaping midlatitude storm tracks. *Journal of the Atmospheric Sciences*, *70*(8), 2596–2613. https://doi.org/10.1175/JAS-D-12-082.1

Kaspi, Y., & Schneider, T. (2011). Downstream self-destruction of strom tracks. *Journal of the Atmospheric Sciences*, *68*(10), 2459–2464. https://doi.org/10.1175/JAS-D-10-05002.1

Kornhuber, K., Petoukhov, V., Petri, S., Rahmstorf, S., & Coumou, D. (2017). Evidence for wave resonance as a key mechanism for generating high-amplitude quasi-stationary waves in boreal summer. *Climate Dynamics*, *49*(5–6), 1961–1979. https://doi.org/10.1007/s00382-016-3399-6

Lee, S. (1995). Localized storm tracks in the absence of local instability. *Journal of the Atmospheric Sciences*, *52*(7), 977–989. https://doi.org/10.1175/1520-0469(1995)052<0977:lstita>2.0.co;2

Luo, D. (2000). Planetary-scale baroclinic envelope Rossby solutions in a two-layer model and their interaction with synoptic-scale eddies. *Dynamics of Atmospheric Ocean*, *32*(1), 27–74. https://doi.org/10.1016/S0377-0265(99)00018-4

Lupo, R. A. (2020). Atmospheric blocking events: A review. *Annals of the New York Academy of Sciences*, *1504*(1), 5–24. https://doi.org/10.1111/nyas.14557

Masato, G., Hoskins, J. B., & Woollings, T. (2011). Wave breaking characteristics of mid-latitude blocking. *Quarterly Journal of the Royal Meteorological Society*, *138*(666), 1285–1296. https://doi.org/10.1002/qj.990

McIntyre, E. M., & Palmer, T. N. (1983). Breaking planetary waves in the stratosphere. *Nature*, *305*(5935), 593–600. https://doi.org/10.1038/305593a0

McIntyre, E. M., Palmer, T. N., & Palmer (1984). The "surf zone" in the stratosphere. *Journal of Atmospheric and Terrestrial Physics*, *46*(9), 825–849. https://doi.org/10.1016/0021-9169(84)90063-1

Mendes, M. C. D., Cavalcanti, I. F., & Herdies, D. L. (2011). Southern Hemisphere atmospheric blocking diagnostic by ECMWF and NCEP/NCAR data. *Revista Brasileira de Meteorologia*, *27*(3), 263–271. https://doi.org/10.1590/S0102-77862012000300001

Michel, C., & Riviére, G. (2011). The link between rossby wave breaking and weather regime transitions. *Journal of the Atmospheric Sciences*, *68*(8), 1730–1748. https://doi.org/10.1175/2011JAS3635.1

Nakamura, H., Nakamura, M., & Anderson, L. J. (1997). The role of high- and low-frequency dynamics in blocking formation. *Monthly Weather Review*, *125*(9), 2074–2093. https://doi.org/10.1175/1520-0493(1997)125<2074:trohal>2.0.co;2

Nakamura, N., & Huang, Y. S. C. (2018). Atmospheric blocking as a trafic jam in the jet stream. *Science*, *361*(6397), 42–47. https://doi.org/10.1126/science.aat0721

Ndarana, T., & Waugh, D. (2010a). The link between cut-off lows and Rossby wave breaking in the Southern Hemisphere. *Quarterly Journal of the Royal Meteorological Society*, *136*(649), 869–885. https://doi.org/10.1002/qj.627

Ndarana, T., & Waugh, W. D. (2010b). A climatology of rossby wave breaking on the southern hemisphere tropopause. *Journal of the Atmospheric Sciences*, *68*(4), 798–811. https://doi.org/10.1175/2010JAS3460.1

O'Brien, L., & Reeder, J. M. (2017). Southern hemisphere summertime rossby waves and Weatherin the Australian region. *Quarterly Journal of the Royal Meteorological Society*, *143*(707), 2374–2388. https://doi.org/10.1002/qj.3090

Patterson, M., Bracegirdle, T., & Woollings, T. (2019). Southern Hemisphere atmospheric blocking CMIP5 and future changes in the Australia-New Zealand sector. *Geophysical Research Letters*, *46*(15), 9281–9290. https://doi.org/10.1029/2019GL083264

Perez, I. (2021). Wind envelope at 300 hPa in the southern hemisphere during austral summer between 1979-2020 (version 1.1) [dataset]. Zenodo. https://doi.org/10.5281/zenodo.7341912

Pérez, I., & Barreiro, M. (2023). Wind envelope amplitude data at 300 hPa for the study of atmospheric waves in the southern hemisphere during austral summer [version 1; peer review: Awaiting peer review]. *Open Research Europe*, *3*(3), 68. https://doi.org/10.12688/openreseurope.15844.1

Pérez, I., Barreiro, M., & Masoller, C. (2021). ENSO and SAM influence on the generation of long episodes of Rossby Wave Packets during Southern Hemisphere summer. *Journal of Geophysical Research: Atmospheres*, *126*(24), e2021JD035467. https://doi.org/10.1029/2021JD035467

Peters, D., & Waugh, W. D. (1996). Influence of barotropic shear on the poleward advection of upper-tropospheric air. *Journal of Atmospheric Science*, *53*(21), 3013–3031. https://doi.org/10.1175/1520-0469(1996)053<3013:iobsot>2.0.co;2

Peters, D., & Waugh, W. D. (2003). Rossby wave breaking in the southern hemisphere wintertime upper troposphere 2003. *Monthly Weather Review*, *131*(11), 2623–2634. https://doi.org/10.1175/1520-0493(2003)131<2623:rwbits>2.0.co;2

Peters, D., & Waugh, W. D. (2003). Rossby wave breaking in the Southern Hemisphere wintertime upper troposphere. *Monthly Weather Review*, *131*(11), 2623–2634. https://doi.org/10.1175/1520-0493(2003)131<2623:rwbits>2.0.co;2

Pinheiro, M. C., Ullrich, P. A., & Grotjahn, R. (2019). Atmospheric blocking and intercomparison of objective detection methods: Flow field characteristics. *Climate Dynamics*, *53*(7–8), 4189–4216. https://doi.org/10.1007/s00382-019-04782-5

Renwick, J. A., & Revell, M. J. (1999). Blocking over the south Pacific and rossby wave propagation. *Monthly Weather Review*, *127*(10), 2233–2247. https://doi.org/10.1175/1520-0493(1999)127<2233:botspa>2.0.co;2

Rex, D. F. (1950). Blocking action in the middle troposphere and its effect upon regional climate. *Tellus*, *2*(3), 196–301. https://doi.org/10.3402/tellusa.v2i4.8603

Rodrigues, R. R., & Woolings, T. (2017). Impact of atmospheric blocking on south America in austral summer. *Journal of Climate*, *30*(5), 1821–1837. https://doi.org/10.1175/jcli-d-16-0493.1

Rossby, C. G. (1945). On the propagation of frequencies and energy in certain types of oceanic, and atmospheric waves. *Journal of Meteorology*, *2*(4), 187–204. https://doi.org/10.1175/1520-0469(1945)002<0187:otpofa>2.0.co;2

Röthlisberger, M., Frossard, L., Bosart, L. F., Keyser, D., & Martius, O. (2019). Recurrent synoptic-scale rossby wave patterns and their effect on the persistence of cold and hot spells. *Journal of Climate*, *32*(11), 3207–3226. https://doi.org/10.1175/jcli-d-18-0664.1

Ryoo, J.-M., Kaspi, Y., Waugh, W. D., Kiladis, N. G., Waliser, E. D., Fetzer, J. E., & Jinwon, K. (2013). Impact of rossby wave breaking on U.S. West coast winter precipitation during ENSO events. *Journal of Climate*, *26*(17), 6360–6382. https://doi.org/10.1175/JCLI-D-12-00297.1

Sagarra, R., & Barreiro, M. (2020). Characterization of extratropical waves during summer of the Southern Hemisphere. *Meteorologica*, *45*(2), 63–79. https://hdl.handle.net/20.500.12008/33550

Simmons, J. A., & Hoskins, J. B. (1978). The life cycles of somenonlinear baroclinic waves. *Journal of the Atmospheric Sciences*, *35*(3), 414–432. https://doi.org/10.1175/1520-0469(1978)035<0414:tlcosn>2.0.co;2

Souders, B. M., Colle, A. B., & Chang, M. K. E. (2014a). The climatology and characteristics of Rossby Wave Packets using a feature-based tracking technique. *Monthly Weather Review*, *142*(10), 3528–3548. https://doi.org/10.1175/MWR-D-13-00371.1

Souders, B. M., Colle, A. B., & Chang, M. K. E. (2014b). A description and evaluation of an automated approach for feature-based tracking of rossby wave packets. *Monthly Weather Review*, *142*(10), 3505–3527. https://doi.org/10.1175/MWR-D-13-00317.1

Strong, C., & Magnusdottir, G. (2008). Trophospheric rossby wave breaking and the NAO/NAM. *Journal of the Atmospheric Sciences*, *65*(9), 2861–2876. https://doi.org/10.1175/2008JAS2632.1

Swanson, K., Kushner, P. J., & Held, M. I. (1997). Dynamics of barotropic storm tracks. *Journal of the Atmospheric Sciences*, *54*(7), 791–810. https://doi.org/10.1175/1520-0469(1997)054<0791:dobst>2.0.co;2

Thorncroft, D. C., Hoskins, J. B., & McIntyre, E. M. (1993). Two paradigms of baroclinic-wave life-cycle behaviour. *Quarterly Journal of Royal Meteorological Society*, *119*(509), 17–55. https://doi.org/10.1002/qj.49711950903

Tibaldi, S., & Molteni, F. (1990). On the operational predictability of blocking. *Tellus*, *42*(3), 343–365. https://doi.org/10.1034/j.1600-0870.1990.t01-2-00003.x

Toulabi Nejad, M., Hejazizadeh, Z., Lupo, A. R., & Saligheh, M. (2022). Spatio-temporal distribution of atmospheric blocking events in the Northern and Southern Hemispheres. *Theoretical and Applied Climatology*, *150*(1–2), 491–505. https://doi.org/10.1007/s00704-022-04175-5

Trenberth, E. K. (1981). Observed southern hemisphere Eddy statistics at 500 mb: Frequency and spatial dependence. *Journal of Atmospheric Science*, *38*(12), 2585–2605. https://doi.org/10.1175/1520-0469(1981)038<2585:oshesa>2.0.co;2

Wang, Y., & Magnusdottir, G. (2010). Tropospheric rossby wave breaking and the SAM. *Journal of Climate*, *24*(8), 2134–2146. https://doi.org/10.1175/2010JCLI4009.1

Weijenborg, C., De Vries, H., & Haarsma, R. J. (2012). On the direction of Rossby wave breaking in blocking. *Climate Dynamics*, *39*(12), 2823–2831. https://doi.org/10.1007/s00382-012-1332-1

Wirth, V. (2020). Wave guidability of idealized midlatitude jets and the limitations of ray tracing theory. *Weather Climate Dynamics*, *1*, 111–125. https://doi.org/10.5194/wcd-1-111-2020

Wirth, V., Riemer, M., Chang, E. K. M., & Martius, O. (2018). Rossby wave packets on the midlatitude waveguide: A review. *Monthly Weather Review*, *146*(7), 1965–2001. https://doi.org/10.1175/MWR-D-16-0483.1

Woollings, T., Barriopedro, D., Methven, J., Son, S.-W., Martius, O., Harvey, B., et al. (2018). Blocking and its response to climate change. *Current Climate Change Reports*, *4*(3), 287–300. https://doi.org/10.1007/s40641-018-0108-z

Yeh, T. C. (1949). On energy dispersion in the atmosphere. *Journal of Meteorology*, *6*(1), 1–16. https://doi.org/10.1175/1520-0469(1949)006<0001:oedita>2.0.co;2

Yeh, T.-C. (1949). On the energy dispersion in the atmosphere. *Journal of the Atmospheric Sciences*, *6*(1), 1–16. https://doi.org/10.1175/1520-0469(1949)006<0001:oedita>2.0.co;2

Zheng, M., Chang, E. K., & Colle, B. A. (2013). Ensemble sensitivity tools for assessing extratropical cyclone intensity and track predictability. *Weather and Forecasting*, *28*(5), 1133–1156. https://doi.org/10.1175/WAF-D-12-00132.1